HHS Public Access

Author manuscript

Oncogene. Author manuscript; available in PMC 2018 November 18.

Published in final edited form as:

Oncogene. 2018 August ; 37(35): 4854–4870. doi:10.1038/s41388-018-0296-y.

NEDD9 promotes oncogenic signaling, a stem/mesenchymal gene signature, and aggressive ovarian cancer growth in mice

Rashid Gabbasov[1,2], **Fang. Xiao**[1], **Caitlin G. Howe**[1], **Laura E. Bickel**[1], **Shane W. O'Brien**[1], **Daniel Benrubi**[3], **Thuy-Vy Do**[1], **Yan Zhou**[4], **Emmanuelle Nicolas**[5], **Kathy Q. Cai**[6], **Samuel Litwin**[4], **Sachiko Seo**[7], **Erica A. Golemis**[1], and **Denise C. Connolly**[1]

[1]Molecular Therapeutics Program, Fox Chase Cancer Center, Philadelphia PA

[2]Kazan Federal University, Department of Biochemistry and Biotechnology

[3]Division of Gynecologic Oncology, Fox Chase Cancer Center, Philadelphia PA

[4]Biostatistics and Bioinformatics Facility, Fox Chase Cancer Center, Philadelphia PA

[5]Genomics Facility, Fox Chase Cancer Center, Philadelphia PA

[6]Histopathology Facility, Fox Chase Cancer Center, Philadelphia PA

[7]Department of Hematology & Oncology, National Cancer Research Center East, Kashiwa, JAPAN

Abstract

Neural precursor cell expressed, developmentally downregulated 9 (NEDD9) supports oncogenic signaling in a number of solid and hematologic tumors. Little is known about the role of NEDD9 in ovarian carcinoma (OC), but available data suggest elevated mRNA and protein expression in advanced stage high grade cancers. We used a transgenic *MISIIR-TAg* mouse OC model combined with genetic ablation of *Nedd9* to investigate its action in the development and progression of OC. A $Nedd9^{-/-}$ genotype delayed tumor growth rate, reduced incidence of ascites, and reduced expression and activation of signaling proteins including SRC, STAT3, E-cadherin and AURKA. Cell lines established from *MISIIR-TAg;*$Nedd9^{-/-}$ and *MISIIR-TAg;*$Nedd9^{+/+}$ mice exhibited altered migration and invasion. Growth of these cells in a syngeneic allograft model indicated that systemic *Nedd9* loss in the microenvironment had little impact on tumor allograft growth, but in a *Nedd9* wild type background $Nedd9^{-/-}$ allografts exhibited significantly reduced growth, dissemination and oncogenic signaling compared to $Nedd9^{+/+}$ allografts. Gene expression analysis revealed that $Nedd9^{+/+}$ tumors exhibited more mesenchymal 'stem-like' transcriptional program, including increased expression of *Aldh1a1* and *Aldh1a2*. Conversely, loss of *Nedd9* resulted in increased expression of differentiation genes, including fallopian tube markers *Foxj1*, *Ovgp1* and *Pax8*. Collectively, these data suggest that tumor cell-intrinsic *Nedd9* expression

Corresponding author: Denise C. Connolly, Ph.D., Molecular Therapeutics Program, 333 Cottman Ave., W310, Philadelphia, PA 19111, Phone: 215-728-1004, FAX: 215-728-2741, Denise.Connolly@fccc.edu.

Conflicts of interest: The authors have no conflicts of interest to declare.

promotes OC development and progression by broad induction of oncogenic protein signaling and stem/mesenchymal gene expression.

Keywords

NEDD9; ovarian carcinoma; metastasis; tumor microenvironment; gene expression

Introduction

Ovarian cancer is the fifth leading cause of cancer mortality and the deadliest gynecologic malignancy[1]. Most malignant ovarian tumors are epithelial in origin and broadly categorized as ovarian carcinoma (OC). OC is often diagnosed at advanced stages with five year survival below 40%[1]. The majority of patients respond to standard treatment (aggressive surgery and cytotoxic chemotherapy), but OC typically reemerges as incurable drug-resistant disease. A deeper understanding of the molecular and cellular mechanisms that contribute to disease development and progression are needed for meaningful improvements in patient outcomes.

Extensive molecular analyses of the most common and lethal subtype of OC, high-grade serous carcinoma (HGSC), reveals nearly ubiquitous mutation of *TP53*, a relatively small subset (10-15%) of cases with mutation of *BRCA1* or *BRCA2*, and high degrees of genomic instability and tumor heterogeneity[2–4]. Mutation of other oncogenes and tumor suppressors occurs at low frequency, making identification of 'actionable' tumor vulnerabilities extremely challenging. Identification of alterations in functional or signaling pathways may be a more tractable way to group tumors by key functions. In this regard, tumor profiling has revealed gene expression signatures that predict outcomes[5,6]. An early study of advanced HGSC identified a unique signature of upregulated genes associated with regulation of motility and invasion, including *NEDD9/HEF1/Cas-L*[7]. NEDD9 is a non-catalytic Crk-associated substrate (CAS) family scaffolding protein that mediates the function of a large number of oncogenic proteins and is of particular interest because of its potential to coordinately regulate a number of metastatic signaling molecules (reviewed in[8]). Via its wide interactome, NEDD9 is involved in fundamental cellular processes, including adhesion, migration, invasion, cell cycle control and survival (reviewed in[8]). Studies performed in solid tumors, leukemias and lymphomas indicate NEDD9 typically promotes tumor growth, but in some tumor types is tumor suppressive (reviewed in[8]). The role of NEDD9 in OC is relatively unexplored, but two studies suggest a tumor-promoting role, with one study identifying elevated *NEDD9* as part of a gene expression signature associated with advanced stage HGSC[7] and a second study finding higher levels of NEDD9 protein expression in invasive OCs[9].

To directly test the role of NEDD9 in OC, we employed genetically engineered mouse (GEM) models, including mice with targeted disruption of *Nedd9*[10] and a transgenic mouse model of spontaneous OC (MISIIR-TAg)[11,12]. MISIIR-TAg mice express the oncogenic SV40 large T (TAg) and small t (tag) antigen genes under control of the Müllerian inhibiting substance type II receptor (MISIIR) gene promoter. Expression of TAg results in functional inactivation of tumor suppressor proteins p53, RB and RB family proteins p107 & p130, and

tag results in inactivation of PP2A, leading to activation of growth-promoting signaling cascades including PI3K/AKT[13]. These alterations are consistent with those most commonly identified human HGSCs, which exhibit nearly ubiquitous mutations in *TP53* (96%), frequent RB pathway inactivation (67%) and elevated PI3K/AKT signaling (45%)[4]. Targeted disruption of *Nedd9* does not affect fertility or viability, but mice exhibit impaired leukocyte adhesion, motility and trafficking via disruption of integrin and receptor signaling[10]. Hence, potential roles for NEDD9 in OC could be tumor cell-intrinsic or alternatively, due to its effects on the tumor microenvironment (TME): a point that has been minimally explored for any cancer. Several studies have demonstrated the presence of tumor infiltrating leukocytes in the OC immune microenvironment, with distinct subclasses having tumor-supportive or -inhibitory effects[14–16]. Thus, NEDD9 could plausibly influence OC development via effects on leukocyte presence and function in the TME. Using newly-established *MISIIR-TAg;Nedd9*$^{-/-}$ and *MISIIR-TAg;Nedd9*$^{+/+}$ murine ovarian carcinoma (MOVCAR) cell lines and a related syngeneic orthotopic OC model[17], we sought to parse the effects of tumor cell-intrinsic and TME-associated loss of *Nedd9* in promoting OC growth *in vivo*. Lastly, as *NEDD9* itself is transcriptionally upregulated in advanced OC[7], we explored the global gene expression profiles of OC tumors isolated from *MISIIR-TAg;Nedd9*$^{-/-}$ and *MISIIR-TAg;Nedd9*$^{+/+}$ mice to determine the effects of *Nedd9* loss on gene expression. Together, our results show a tumor-promoting role for NEDD9 that is largely or entirely tumor cell-intrinsic and mediated by increased oncogenic signaling and a prominent shift toward more mesenchymal, stem-like gene expression.

Results

Deletion of *Nedd9* delays development of ovarian tumors

To determine the effect of genetic ablation of *Nedd9* in OC, transgenic *MISIIR-TAg* mice[11,12] were crossed to *Nedd9*$^{-/-}$ mice[10] and ovarian volume (tumor growth) was monitored and quantified in age-matched female *MISIIR-TAg;Nedd9*$^{-/-}$ (n=27) and *MISIIR-TAg;Nedd9*$^{+/+}$ (n=24) mice by longitudinal *in vivo* magnetic resonance imaging (MRI)[12,18]. Tumor initiation begins early in *MISIIR-TAg* mice[12], with TAg positive tumor cells present within normal sized ovaries of 4-8 week old mice (Supplementary Figure S1), and evidence of ovarian enlargement due to the presence of tumor beginning around 12 weeks of age. Thus, mice received baseline scans when the mean age was 11-12 weeks and 2-10 additional scans, with the endpoint defined as the point at which tumor volume or lack of animal wellness met humane criteria for euthanasia. Baseline MRI revealed a small difference in mean ovarian volume in age-matched mice (Fig. 1A and Table 1). Linear mixed-effects models with random intercepts were used to model longitudinal log-transformed volume data from the first three MRI scans, when all 51 mice were alive. Models included fixed effects for time, group and time by group interaction. The interaction of group and time, included to determine if the group effect varied significantly over time, was not statistically significant. In contrast, when the model was fit to the data without the interaction term, a significantly lower mean log-transformed volume was observed for *MISIIR-TAg;Nedd9*$^{-/-}$ mice compared to *MISIIR-TAg;Nedd9*$^{+/+}$ controls at the third scan, when the mice were 15 weeks old ($p=0.035$, Fig. 1B and Table 1). Tumor growth slopes calculated for each individual mouse over the duration of the study revealed an overall delay

in tumor growth rate in *MISIIR-TAg;Nedd9*$^{-/-}$ mice that closely approached significance (p=0.054, Fig. 1C). Endpoint data including age, final tumor volume, presence of ascites and gross and microscopic evidence of disease spread are summarized in Table 2. Abdominal ascites, a common feature of *MISIIR-TAg* mice[11,18], was detected less frequently in *MISIIR-TAg;Nedd9*$^{-/-}$ mice (Fig. 1D and Table 2), but the trend did not reach significance. Histology, expression of TAg and common HGSC markers PAX8 or WT1 revealed no obvious genotype-associated differences at study endpoint or at early stage (Fig. 1E and Supplemental Figure S1A).

There were no genotype-specific differences in tumor dissemination. All mice exhibited spread of tumor cells to omentum and over half showed evidence of infiltration of lung; invasive lesions in kidney, liver, intestine or pancreas were rare events in either genotype (Supplementary Tables S1 & S2, and Supplementary Fig. S1B&C). Similarly, no genotype-specific differences in the presence or extent of early lesions were observed; all young mice (4, 8, and 12 weeks old) exhibited oviductal (the murine equivalent of fallopian tube) epithelial atypia that increased in severity with age, and was similar to tubal intraepithelial carcinoma (TIC) and tubal carcinoma (TC) lesions detected in women with HGSC. There was an age-dependent increase in the presence of TAg+ tumor cells in the ovaries, and TAg+ tumor cells were occasionally observed in the hilum, the ovarian surface epithelium, and the epithelial cells lining paraovarian and/or ovarian inclusion cysts (Supplementary Table S3 and Supplementary Fig. S2). Similarly, an age-dependent increase in *TAg* and *Nedd9* gene expression was observed in *MISIIR-TAg* mice (Supplementary Fig. S3C). Together, these results show that loss of *Nedd9* delays early tumor growth rate and may limit the development of ascites, but suggest that compensatory mechanisms may overcome *Nedd9* loss in this aggressive mouse model of OC.

Loss of *Nedd9* disrupts oncogenic signaling in ovarian tumors

To understand the mechanisms that contribute to the delayed tumor growth in *MISIIR-TAg;Nedd9*$^{-/-}$ mice, expression and activation of a large panel of known NEDD9 interacting proteins were evaluated in tumor lysates of both genotypes (Fig. 2, Supplementary Fig. S4). Src activation was diminished in tumors from *MISIIR-TAg;Nedd9*$^{-/-}$ mice, as evidenced by the reduction of the activated (pSrc^{Y416}) and increase in auto-inhibited (pSrc^{Y527}) forms of Src. Levels of activated pFAK^{Y397} and pFAK^{Y861} were reduced in some cases, but this was less consistent (Supplementary Fig. S4). STAT3 activation (pSTAT3^{Y705}), often elevated in aggressive OCs, was reduced in tumors from *MISIIR-TAg;Nedd9*$^{-/-}$ mice (Fig. 2). Tumors from *MISIIR-TAg;Nedd9*$^{-/-}$ mice also exhibited reduced levels of AURKA and E-cadherin (Fig. 2), proteins that support OC proliferation and survival[19,20]. In contrast, AKT, ERK, and N-cadherin showed no consistent differences in patterns of expression and/or activation (Supplementary Fig. S4). Induction of compensatory signaling mechanisms may support tumor growth in mice with deletion of *Nedd9*. An obvious candidate is p130Cas/BCAR1, a structural and functional paralogue of *NEDD9*[21]; however, similar levels of p130Cas/BCAR1 were observed regardless of genotype (Fig. 2).

Loss of *Nedd9* alters *in vitro* migration and invasion of OC cells

To enable further study of the effects of loss of *Nedd9* on properties of ovarian oncogenesis, murine ovarian carcinoma (MOVCAR) cell cultures were derived from malignant cells present in ascites collected from mice. Four independent *MISIIR-TAg;Nedd9*$^{+/+}$ and *MISIIR-TAg;Nedd9*$^{-/-}$ tumor cell lines, whose OC origin was validated by TAg and cytokeratin expression and the presence/absence of NEDD9 protein (Supplementary Fig. S5A), were used to evaluate proliferation, adhesion, migration and invasion. No *Nedd9* genotype-associated differences were observed in proliferation or in adhesion to type I collagen or fibronectin (Supplementary Fig. S5B-C). Real-time analysis of cell migration through transwell membranes showed an increased mean migration rate of *Nedd9*$^{-/-}$ cells in the absence of serum, but no differences in the presence of serum (Fig. 3A-B and Supplementary Fig. S5D). Additionally, *Nedd9*$^{-/-}$ cells invaded through 3D basement membrane significantly faster than controls, regardless of the presence of serum (Fig. 3C-D and Supplementary Fig. S5E). Wound closure and single cell motility analyses confirmed increased migration in *Nedd9*$^{-/-}$ cells compared to wild type controls (Fig. 3E-F and Supplementary Figs. S5F-H & S6). Depletion of wild type *NEDD9* in MOVCAR and human OC cell lines (n=2 independent cell lines for each) showed results consistent with the *Nedd9*$^{-/-}$ ascites-derived MOVCAR cells, where shRNA-mediated depletion of *NEDD9* significantly enhanced wound closure for all cell lines tested (Fig. 3G).

The enhanced migration and invasion observed in cultured *Nedd9*$^{-/-}$ cells was somewhat paradoxical in light of the delay in early tumor growth observed in *MISIIR-TAg;Nedd9*$^{-/-}$ mice *in vivo* (Fig. 1). Interestingly, analysis of NEDD9 interacting proteins revealed key differences in cultured cells compared to tumors; pFAK^{Y397}and pSTAT3^{Y705} levels were significantly increased in 2D cultured *Nedd9*$^{-/-}$ cells compared to *Nedd9*$^{+/+}$ control cells (Fig. 3H). Activation of these proteins could support the enhanced migration and invasion observed in cells *in vitro*.

Nedd9 in the microenvironment is not required for OC growth and dissemination

Nedd9$^{-/-}$ mice have defects in migration and trafficking of B and T lymphocytes to secondary lymphoid organs[10]. To determine if this or other NEDD9-mediated aspects of the TME contribute to OC we compared the effects of *Nedd9* loss in the microenvironment on the growth of *Nedd9*$^{+/+}$ MOVCAR cells *in vivo* in an immunocompetent orthotopic allograft model[17]. Female *MISIIR-TAg-low* mice do not develop tumors, but are permissive syngeneic hosts for growth of TAg-expressing MOVCAR cells due to low level TAg expression in the oviductal epithelium[17]. In contrast to the result with the *MISIIR-TAg* model, ovaries isolated from 4 and 14 week-old *MISIIR-TAg-low* mice exhibit similar levels of NEDD9 and no detectable TAg expression (Supplementary Fig. S3). *MISIIR-TAg-low;Nedd9*$^{-/-}$ and *MISIIR-TAg-low;Nedd9*$^{+/+}$ mice received unilateral intrabursal implantation of luciferase-expressing *Nedd9*$^{+/+}$ MOVCAR-5009-luc cells (Fig. 4A). Longitudinal bioluminescent imaging (BLI) showed no significant difference in luciferase expression from tumors in mice of either genotype (Fig. 4B). Mice from both groups reached humane criteria for euthanasia within the same time-frame (53.1±1.7 days for *MISIIR-TAg-low;Nedd9*$^{+/+}$ vs. 52.8±1.9 days for *MISIIR-TAg-low;Nedd9*$^{-/-}$ mice), and no significant differences in primary tumor volume, the number or volume of tumor nodules,

incidence of ascites or tumor histology (Fig. 4C-G). Protein lysates from MOVCAR-5009-luc tumors grown in *MISIIR-TAg-low;Nedd9*$^{-/-}$ and *MISIIR-TAg-low;Nedd9*$^{+/+}$ hosts exhibited no consistent differences in expression or phosphorylation of oncogenic proteins analyzed (data not shown). Finally, detailed analysis of leukocyte populations detected in primary tumors, lymph nodes and peritoneal washes of *MISIIR-TAg-low;Nedd9*$^{-/-}$ and *MISIIR-TAg-low;Nedd9*$^{+/+}$ hosts revealed significantly fewer CD45^{+}NK1.1^{+}CD3e^{+} natural killer cells in the peritoneal cavities of *MISIIR-TAg-low;Nedd9*$^{-/-}$ mice, but no significant differences in other leukocyte populations analyzed at any other site (Supplementary Table S4 and Fig. S7). Together, these results strongly suggest that the loss of *Nedd9* in the host has no significant impact on leukocyte infiltration of OC tumors, the peritoneal environment, or other aspects of the TME that affect the growth or progression of orthotopic tumors. Thus, differences in spontaneous tumor growth in *MISIIR-TAg;Nedd9*$^{-/-}$ and *MISIIR-TAg;Nedd9*$^{+/+}$ control mice are likely tumor cell-intrinsic.

Tumor cell-intrinsic *Nedd9* expression promotes OC growth and dissemination

To determine whether the aggressive characteristics of *Nedd9*$^{-/-}$ MOVCAR cells observed *in vitro* are maintained *in vivo*, we compared tumor growth and dissemination in *TAg-Low;Nedd9*$^{+/+}$ hosts harboring orthotopic allografts of *Nedd9*$^{-/-}$ and *Nedd9*$^{+/+}$ MOVCAR cells (Fig. 5A). Strikingly, unlike hyperaggressive tumor cell lines derived from *Nedd9*$^{-/-}$ mammary carcinomas[22,23], allografts derived from *Nedd9*$^{-/-}$ cells grew more slowly than those derived from *Nedd9*$^{+/+}$ cells (Fig. 5B-E). Moreover, there was a dramatic difference in tumor dissemination in *Nedd9*$^{-/-}$ mice, as evidenced by highly significant decreases in the average number of tumor nodules, ascites incidence and ascites volume in mice harboring *Nedd9*$^{-/-}$ compared to *Nedd9*$^{+/+}$ controls (Fig. 5G-I). Western blot analysis performed on tumor cell lysates showed decreased expression and/or activation of oncogenic proteins in *Nedd9*$^{-/-}$ tumors (Fig. 5J), including total and activated FAK and STAT3 and E-cadherin. These results strongly support the initial observations in spontaneous tumors from transgenic mice, demonstrating prominent effects of loss of *Nedd9* in OC cells, including delayed tumor growth and decreased tumor dissemination and ascites production.

Loss of Nedd9 alters gene expression

To further investigate the potential mechanisms of NEDD9 action in OC, we performed genome wide mRNA microarray analysis of tumors isolated from *MISIIR-TAg;Nedd9*$^{+/+}$ and *MISIIR-TAg;Nedd9*$^{-/-}$ mice (n = 4 tumors of each genotype). Application of strict criteria of a 2-fold change and a false discovery rate (FDR) of 5% identified a subset of 46 genes as the most differentially regulated between the two groups (Fig. 6A and Supplementary Table S5). Among these, 36 genes were upregulated and 10 genes were downregulated in *Nedd9*$^{-/-}$ compared to *Nedd9*$^{+/+}$ control tumors. Consistent with genotype, *Nedd9* was among the most significantly downregulated genes in *Nedd9*$^{-/-}$ tumors (Fig. 6A). Expression of *Nedd9* and a subset of seven genes were independently analyzed by qRT-PCR, validating differential expression for all but *Atp2b2* (Fig. 6B and data not shown). Notable among the genes upregulated in *Nedd9*$^{-/-}$ tumors were *Bmpr1b* and *Foxj1*, both of which were previously shown to be downregulated in human OCs[24,25]. Expression of both genes was increased in individual *Nedd9*$^{-/-}$ tumors, and elevated protein

expression was detected for FOXJ1 (Fig. 6B-C), a member of the forkhead box family of transcription factors.

FOXJ1 is a potent regulator of the transcriptional program controlling the production of motile cilia, and a marker of ciliated cells of the fallopian tube epithelium (FTE)[26]. Upregulation of *Foxj1* in tumors pointed to tissue-specific gene expression related to ciliated FTE differentiation. Consistent with this, analysis of the data set with more relaxed statistical cutoff (FDR<20%, 4-fold change cutoff, Supplementary Table S6) via the Gene Ontology (GO) database showed significant enrichment of genes with biological processes involved in the assembly and function of motile cilia, including axoneme and inner and outer dynein arm assembly, cilium assembly, movement, organization, morphogenesis and beat frequency (Supplementary Table S7). Differential expression of *Foxj1* and eight known FOXJ1 transcriptional targets associated with motile ciliogenesis[27], six of which were present in our extended list, was independently validated by qRT-PCR (Fig. 6D). Interestingly, analysis of the dataset also revealed significantly increased expression of *Pax8* and *Ovgp1*, genes characteristically expressed in secretory FTE cells, the putative cell of origin of human HGSCs[28–31] (Fig. 6C, D&H). Examination of normal oviducts in $Nedd9^{-/-}$ and $Nedd9^{+/+}$ mice showed no apparent differences in the proportions of ciliated or secretory FTE (Supplementary Fig. S8). Therefore, the overexpression of several FTE-specific genes in $Nedd9^{-/-}$ tumors suggests that in the absence of *Nedd9*, ovarian tumors may exhibit gene expression profiles consistent with a more differentiated phenotype.

Recent work using Gene Set Enrichment Analysis (GSEA) identified a ‘stem cell-like’ gene expression signature in poorly differentiated aggressive tumors that is highly correlated with genes expressed in embryonic stem cells[32]. A subsequent study using this methodology defined a 51-gene ‘stem cell-like’ signature in HGSC[33]. Comparison of differentially expressed genes in the $Nedd9^{-/-}$ *vs.* $Nedd9^{+/+}$ dataset (4969 significant genes (FDR20, FC1.5) among the total 24,345 known genes on the array) to the 51-gene stem cell-like gene signature showed significant overlap (Fisher’s exact test). Among the 51-gene human signature, a total of 43 homologous murine probes were identified, with 22/43 (51.1%, p=7.2 e-06) overlapping between the two datasets (Fig. 6E). To further explore the relationship of *Nedd9* loss and FTE gene expression, we similarly compared our dataset with a 78-gene stem cell gene signature recently described in human fallopian tube (FT) organoids[34]. Maintenance of stem cell gene expression in FT organoids is Notch-dependent, with Notch inhibition decreasing expression of stem cell genes and increasing expression of genes associated with differentiation, including *FOXJ1*[34]. Comparison of the murine *Nedd9* dataset with the FT stem cell signature showed very significant overlap, with 38/77 (49.4%, p=1.4 e-08) homologous probes overlapping (Fig. 6F).

The 78-gene stem cell-associated signature for FT organoids was defined by identifying the subset of genes significantly enriched within a 384 gene stem cell signature previously defined in $LGR5^+$ cells in murine intestinal crypt[35]. We also compared the overlap between the *Nedd9* dataset and the murine $LGR5^+$ intestinal crypt stem cell signature, and again found highly significant overlap of 156/384 (40.6%, p=2.2 e-16) genes (Fig. 6G). A subset of overlapping genes identified in these datasets, selected based on their known expression in FTE (*Pax8* and *Ovgp1*), putative role as OC stem cell markers (*Aldh1a1*, *Aldh1a2* and

CD44), or presence in the OC stem cell signature (*Slc14a1* and *Scl1a1*) or fallopian tube stem cell signature (*Armc4* and *Lrrc6*), were validated by qRT-PCR (Fig. 6H). Together, these comparisons support the idea that loss of *Nedd9* results in a shift in transcriptional program from a less differentiated more mesenchymal 'stem cell-like' profile to a more differentiated profile of gene expression in murine OC. These data also demonstrate relationship of gene expression profiles between murine *MISIIR-TAg* OCs and fallopian tube, a preferred site of origin of human HGSCs[30].

Discussion

Elevated NEDD9 expression has been identified as a biomarker of aggressive human tumors, including melanoma, GBM, breast and lung cancers[36–39] (and reviewed in[8]). While NEDD9 has generally been identified as a promoter of cancer cell aggressiveness, one study reported downregulation of *NEDD9* as part of a gene expression signature predicting breast cancer cell metastasis to lung[40]. In a p210*Bcr/Abl* mouse model of chronic myelogenous leukemia (CML), loss of *Nedd9* accelerated the development of CML/myeloproliferative neoplasm, increased infiltration of myeloid cells in several tissues and decreased overall survival[41]. These disparate observations suggest that the role of NEDD9 in cancer is likely tissue- and context-dependent. Analysis of OC clinical specimens and TCGA data (Supplementary Fig. S3) suggests overexpression of *NEDD9* mRNA and protein is correlated with more advanced cancers and unfavorable prognosis[4,42]; however to date, the functional role of NEDD9 in OC has not been explored. The results of this study show for the first time the effects of genetic ablation of *Nedd9* in an aggressive transgenic model of OC. Our results reveal that loss of *Nedd9* did not abrogate tumor development, but resulted in a pronounced delay in tumor growth rate most apparent in young mice. Moreover, the frequency of malignant ascites development was reduced in mice lacking *Nedd9*. These observations led us to conclude that *Nedd9* is not absolutely required for OC, but promotes OC growth and progression.

As *Nedd9* has multiple functions, there are multiple avenues by which its loss of function can influence tumorigenesis. First, is via its well-established function as a scaffold protein that activates key oncogenic signaling proteins. In spontaneous tumors or allografts lacking *Nedd9*, expression or activation of Src, AURKA and STAT3, was reduced, and in *Nedd9*$^{-/-}$ allografts, FAK activation was also diminished. We and others have shown that each of these proteins support ovarian tumorigenesis[18,19,43–46]. The novel association between NEDD9 and STAT3 activation we report is consistent with tumor growth inhibition as our prior work demonstrated that targeted blockade of JAK/STAT3 in *MISIIR-TAg* mice inhibited OC development[18]. The reduction of E-cadherin in the absence of *Nedd9* is different from most other tumor models[8] and may seem inconsistent with the gene expression data suggesting a shift from more mesenchymal 'stem cell-like' toward more differentiated gene expression; however, in OC the production of malignant ascites and multicellular aggregates, key mechanisms of OC dissemination, are associated with high levels of E-cadherin expression[20,47]. Thus, reduction of E-cadherin levels in *MISIIR-TAg;Nedd9*$^{-/-}$ mice and in *Nedd9*$^{-/-}$ allografts in *MISIIR-TAg-Low* mice likely underlies the reduced ascites production and dissemination observed.

Interestingly, in mice that are *Nedd9*$^{-/-}$, but lack the presence of a driver oncogene, the most notable observed defects were impaired lymphocyte motility and trafficking, with diminished chemotactic migration response of splenic B and T cells to CXCL12[10]. The importance of CXCL12 signaling axis in OC is well-established[48], and analysis of this and other cytokine/chemokine expression in our models merits further study. The presence of tumor infiltrating lymphocytes (TILs) or T regulatory (T_{Reg}) cells in patient tumors is correlated with better and worse prognosis, respectively[14–16]. Notably, we have shown that blockade of JAK/STAT3 signaling in *MISIIR-TAg* mice inhibited OC development in part by reducing T_{Reg} cells in the peritoneal TME[18]. Thus, it was important to investigate the effects of loss of *Nedd9* in the TME. However, our results provide convincing evidence that OC growth and dissemination in this model is not affected by loss of *Nedd9* in the TME, instead supporting tumor-cell intrinsic effects.

Our *in vivo* findings are consistent with the *MMTV-PyVmT* mammary carcinoma model, where *Nedd9* loss delayed tumor onset and decreased tumor multiplicity, but did not abrogate tumor development or progression[22]. In this model, loss of *Nedd9* had prominent effects on NEDD9-regulated signaling proteins including SRC, FAK, Shc and AKT. Tumor-derived cell lines lacking *Nedd9* showed increased anchorage-independent growth, 3D growth on matrices, and increased formation of orthotopic allografts and metastatic spread compared to *Nedd9*$^{+/+}$ controls suggesting selection of cells with hyperaggressive characteristics[23]. The increased migration and invasion capacity observed in *Nedd9*$^{-/-}$ MOVCAR cells might similarly indicate hyperaggressive clonal outgrowths from *Nedd9*$^{-/-}$ OCs; however, when cells were grown *in vivo*, tumor latency increased and dissemination was significantly impaired. Thus, *in vivo* results confirm decreased tumorigenic potential in the absence of *Nedd9*. The basis for the difference in behavior *in vitro* and *in vivo* is unknown, but may be attributable to cell culture conditions[49].

Accumulating evidence suggests that phenotypic behaviors (e.g., proliferation, drug response, migration, etc.) of cancer cells grown in 2D culture can be quite different from cells grown in 3D culture as spheroids, 3D organotypic cultures, or as tumors in vivo[50]. This may be particularly true for OC cells as these cells typically disseminate as clusters. Of critical importance to cell survival *in vivo* may be alterations in proteins and/or signaling pathways that protect cells from anoikis[51]. Notably, levels of E-cadherin, activated Src ($pSRC^{Y416}$) and FAK ($pFAK^{Y397}$), known to protect cells from anoikis, are diminished in primary *Nedd9*$^{-/-}$ tumors and/or *Nedd9*$^{-/-}$ MOVCAR allografts.

Loss of *Nedd9* in the MMTV-Neu mammary cancer model had a more dramatic effect, limiting the incidence of tumors and increasing latency[52]. Unlike the *MMTV-PyVmT* or *MISIIR-TAg* models, there were no consistent effects on NEDD9-regulated signaling proteins/pathways, and also unlike our OC model, there was little difference in gene expression between *Nedd9* wild type and null *MMTV-Neu* tumors[22,52]. The underlying defect in this model was a reduction in the number of luminal epithelial progenitors. The connection to progenitor cells is intriguing in the context of OC; however, this cannot be adequately studied as consensus regarding the progenitor cell of HGSCs in humans or mice is lacking. Together, observations in *MISIIR-TAg* and other mouse models lacking *Nedd9* underscore the idea that its function is highly tissue- and context-dependent.

NEDD9 is associated with epithelial-to-mesenchymal transition in multiple tumor types (reviewed in[8,53]). Transcriptional profiling data showed significant differences between *Nedd9* null and wild type tumors, with strong overlap of stem-cell-like signatures[33,35,54], supporting an more mesenchymal 'stem-like' gene expression in *Nedd9* wild type tumors and expression of genes associated with a differentiated phenotype in *Nedd9* null tumors. Particularly striking was the downregulation of putative ovarian cancer stem cell markers (*ALDH1A1, ALDH1A2* and *CD44*) and upregulation of common markers of FTE differentiation (*PAX8*, *OVGP1* and *FOXJ1*) as well as a plethora of *FOXJ1*-regulated genes associated with ciliogenesis. Notably, altered expression of *NANOG*, a transcription factor required for stem cell renewal and pluripotency, has inverse effects on FOXJ1 expression in OC[25]. Over the past decade there has been a significant paradigm shift with the recognition that HGSC of the ovary likely arise in the FTE[30]. The altered expression of stem cell and FTE differentiation markers underscores the connection of NEDD9 in OC in the MISIIR-TAg model and provides *in vivo* evidence supporting a pro-tumorigenic role for NEDD9 in human HGSC.

Materials and methods

Mouse strains, breeding and tumor induction

Procedures involving mice were approved by the FCCC IACUC. C57BL/6J *MISIIR-TAg* and *MISIIR-TAg-low* mouse strains were developed in our laboratory and described previously[11,12,17]. *MISIIR-TAg* mice develop spontaneous bilateral ovarian tumors and *MISIIR-TAg-low* mice express *TAg* at low levels in the oviduct, do not develop ovarian tumors, and are permissive syngeneic hosts for allograft implantation of murine ovarian carcinoma (MOVCAR) cells isolated from *MISIIR-TAg* mice[17]. C57BL/6J *Nedd9*$^{-/-}$ mice were previously described[10]. Male *MISIIR-TAg* and *MISIIR-TAg-low* mice were crossed with female *Nedd9*$^{-/-}$ mice to obtain *MISIIR-TAg/TAg-low*;*Nedd9*$^{+/-}$ offspring and males were crossed with *Nedd9*$^{-/-}$ females to generate *MISIIR-TAg*;*Nedd9*$^{-/-}$ and *MISIIR-TAg-low*;*Nedd9*$^{-/-}$ mice. Tumor allografts were implanted in age-matched (13-15 week-old) MISIIR-TAg-low mice unilateral intrabursal injection of 3×10^5 luciferase expressing cells as described[17,55].

Longitudinal *in vivo* tumor imaging

In vivo tumor imaging was performed in the FCCC Biological Imaging Facility and growth of spontaneous ovarian tumors in transgenic mice was monitored and quantified by magnetic resonance imaging (MRI) as described[12,55]. Mice received baseline images starting at approximately 10-12 weeks of age and were imaged biweekly (early stages) or weekly (later stages) for an additional 4-17 weeks. The study endpoint was set at the point at which individual mice reached IACUC-approved humane criteria for euthanasia, typically based on tumor volume or lack of wellness. Growth of orthotopic allografts was monitored by weekly bioluminescent imaging (BLI)[17,55] with the same definition of study endpoint.

Tumor collection, tissue preparation and analysis

Mice were euthanized by CO_2 inhalation and necropsied. Tumor volume ($l \times w^2 \times 0.5$) and the presence and number of tumor nodules was noted and affected tissues and portions of

normal organs were collected and snap frozen or fixed in 10% neutral buffered formalin, paraffin embedded then sectioned for H&E staining and immunohistochemical detection of TAg, PAX8 and WT1 as described[11].

Cell lines and culture conditions and antibodies

MOVCAR cell lines were derived from the ascites of *MISIIR-TAg*;*Nedd9*$^{+/+}$ (MOVCAR-5009, -6111, -7577, -8248, -8250) and *MISIIR-TAg*;*Nedd9*$^{-/-}$ (MOVCAR-136, -143, -145, -168) mice in our laboratory as described[12]. Human OC cell lines OVCAR-5 and A1847 OC were obtained from the FCCC Cell Culture Facility (deposited by Dr. Thomas Hamilton) and maintained as described[56]. Cell lines were periodically checked for mycoplasma contamination OVCAR-5 cells were authenticated by STR profiling. Antibodies and commercial source: antibodies recognizing AKT (cat# 468S), pAKT^{S473} (cat# 3787S), ERK 1/2 (9102), pERK1/2$^{T202\text{-}Y204}$ (cat# 9106S), Src (cat# 2108S), pSrc^{Y416} (cat# 2101S), pSrc^{Y527} (2105S), STAT3 (cat# 9132) and pSTAT3^{Y705} (cat# 9145S), pan-keratin (cat# 4545) (Cell Signaling Technology; Danvers, MA, USA), NEDD9 (cat# ab18056) (Abcam; Cambridge, MA, USA), SV40-TAg (cat# sc-147), β-actin (cat# sc-8432), E-cadherin (cat# sc-7870), N-cadherin (cat# sc-7939), p130Cas (cat# sc-860) (Santa Cruz Biotechnology; Santa Cruz, CA, USA), BMPR1B (cat# bs-6639R), and FOXJ1 (cat# 36887) (One World Lab; San Diego, CA, USA), and PAX8 (cat# 10336-I-AP) (Proteintech Group, Rosemont, IL, USA).

Immunoblot, migration and invasion assays

Cell and tumor tissue lysates, protein assays and Western analysis performed as described[56]. Transwell migration and invasion assays were performed using the xCELLigence system (Roche, Basel, Switzerland) for real-time cell analysis (RTCA) using Roche cellular invasion/migration (CIM)-plates according to manufacturer's instructions and described in detail in Supplementary Methods.

In vitro knockdown of *NEDD9*

NEDD9 was depleted by lentiviral transduction of short hairpin RNA constructs targeting human (pGIPZ, GE Dharmacon; Lafayette, CO, USA) or murine (pLKO.1, GE Dharmacon) *NEDD9* (shRNA sequences in Supplementary Table S8). Lentivirus was generated using HEK293T cells and Virapower Kit (Invitrogen, now Thermo Fisher Scientific; Waltham, MA, USA) and filtered medium used to infect target cells. Transduced cells were selected with puromycin. Empty vector was used as negative control and shRNAs targeting *GAPDH* and *eGFP* were used as non-specific controls for human and mouse lines respectively.

Gene expression analysis and quantitative RT-PCR

Tumor RNA was isolated and submitted to the FCCC Genomics Facility for gene expression analyses by microarray and quantitative RT-PCR as described in detail in[18] and Supplementary Methods. Raw and normalized data are accessible through Gene Expression Omnibus accession number GSE106911. Differentially expressed genes were identified based on statistical significance (FDR<0.05) and biological significance using a fold-change cutoff of 2. Fisher's exact test was used to test whether there is significant association

between the murine NEDD9 essential genes from our study to those in previously published datasets[33–35]. Differential expression of individual genes was validated by qRT-PCR amplification as described[18] using Power SYBR Green (Invitrogen, now Thermo Fisher Scientific) and gene specific-probes (Supplementary Table S9) or Taqman technology and probes (Invitrogen, now Thermo Fisher Scientific, Supplementary Table S10) with *Ppib* and *Hprt1* as normalizer genes.

Statistical Analysis

Data were submitted to the Biostatics and Bioinformatics Facility for analysis. Wilcoxon two-sample two-sided tests were used to analyze the *in vitro* data. Specific analyses are also described in the results and figure legends. Multiple comparisons were not adjusted. For all analyses, p values of <0.05 were considered significant.

Supplementary Material

Refer to Web version on PubMed Central for supplementary material.

Acknowledgments

The authors gratefully acknowledge Drs. Zeng-jie Yang and David Schlaepfer for helpful discussions; Dr. Eric Ross and Ms. Ludmilla Demora of the FCCC Biostatistics and Bioinformatics Facility for helpful discussions and statistical analysis; Ms. Ellen Neulight for assistance with genotyping transgenic mice; Ms. Jane Miglo for technical assistance; and Mr. Xiang Hua in the Transgenic Mouse Facility for assistance with intrabursal injections. This work was supported by the FCCC Laboratory Animal, High Throughput Screening, Cell Culture, Biosample Repository, Biomedical Imaging, Histopathology, Transgenic Mouse and Biostatistics and Bioinformatics Facilities.

Financial Support: This work was supported by R01 CA136596 (to DCC); R01 CA63366 (to EAG); Ovarian SPORE P50 CA083638, the FCCC Core Grant NCI P30 CA006927, and charitable donations from the Roberta Dubrow Fund, the Teal Tea Foundation, and the Bucks County Board of Associates (to DCC).

Grant Support

This work was supported supported by R01 CA136596 (to DCC), R01 CA63366 (to EAG), and the FCCC Core Grant NCI P30 CA006927 as well as charitable donations (to D.C.C.'s laboratory) from the Roberta Dubrow Fund, the Teal Tea Foundation, the Bucks County Board of Associates and the Main Line Board of Associates.

References

1. Siegel RL, Miller KD, Jemal A. Cancer statistics, 2016. CA: A Cancer Journal for Clinicians. 2016; 66(1):7–30. [PubMed: 26742998]
2. Bowtell DD, Bohm S, Ahmed AA, Aspuria PJ, Bast RC Jr, Beral V, et al. Rethinking ovarian cancer II: reducing mortality from high-grade serous ovarian cancer. Nat Rev Cancer. 2015; 15(11):668–79. [PubMed: 26493647]
3. McPherson A, Roth A, Laks E, Masud T, Bashashati A, Zhang AW, et al. Divergent modes of clonal spread and intraperitoneal mixing in high-grade serous ovarian cancer. Nat Genet. 2016; 48(7):758–67. [PubMed: 27182968]
4. TCGA. Integrated genomic analyses of ovarian carcinoma. Nature. 2011; 474(7353):609–15. [PubMed: 21720365]
5. Bonome T, Levine DA, Shih J, Randonovich M, Pise-Masison CA, Bogomolniy F, et al. A gene signature predicting for survival in suboptimally debulked patients with ovarian cancer. Cancer Res. 2008; 68(13):5478–86. [PubMed: 18593951]
6. Verhaak RG, Tamayo P, Yang JY, Hubbard D, Zhang H, Creighton CJ, et al. Prognostically relevant gene signatures of high-grade serous ovarian carcinoma. J Clin Invest. 2013; 123(1):517–25. [PubMed: 23257362]

7. Donninger H, Bonome T, Radonovich M, Pise-Masison CA, Brady J, Shih JH, et al. Whole genome expression profiling of advance stage papillary serous ovarian cancer reveals activated pathways. Oncogene. 2004; 23(49):8065–77. [PubMed: 15361855]
8. Shagisultanova E, Gaponova AV, Gabbasov R, Nicolas E, Golemis EA. Preclinical and clinical studies of the NEDD9 scaffold protein in cancer and other diseases. Gene. 2015; 567(1):1–11. [PubMed: 25967390]
9. Wang H, Mu X, Zhou S, Zhang J, Dai J, Tang L, et al. NEDD9 overexpression is associated with the progression of and an unfavorable prognosis in epithelial ovarian cancer. Hum Pathol. 2014; 45(2): 401–8. [PubMed: 24439227]
10. Seo S, Asai T, Saito T, Suzuki T, Morishita Y, Nakamoto T, et al. Crk-associated substrate lymphocyte type is required for lymphocyte trafficking and marginal zone B cell maintenance. J Immunol. 2005; 175(6):3492–501. [PubMed: 16148091]
11. Connolly DC, Bao R, Nikitin AY, Stephens KC, Poole TW, Hua X, et al. Female mice chimeric for expression of the simian virus 40 TAg under control of the MISIIR promoter develop epithelial ovarian cancer. Cancer Res. 2003; 63(6):1389–97. [PubMed: 12649204]
12. Hensley H, Quinn BA, Wolf RL, Litwin SL, Mabuchi S, Williams SJ, et al. Magnetic Resonance Imaging for Detection and Determination of Tumor Volume in a Genetically Engineered Mouse Model of Ovarian Cancer. Cancer Biol Ther. 2007; 6(11)
13. Colvin EK, Weir C, Ikin RJ, Hudson AL. SV40 TAg mouse models of cancer. Semin Cell Dev Biol. 2014; 27:61–73. [PubMed: 24583142]
14. Curiel TJ, Coukos G, Zou L, Alvarez X, Cheng P, Mottram P, et al. Specific recruitment of regulatory T cells in ovarian carcinoma fosters immune privilege and predicts reduced survival. Nat Med. 2004; 10(9):942–9. [PubMed: 15322536]
15. Facciabene A, Motz GT, Coukos G. T-regulatory cells: key players in tumor immune escape and angiogenesis. Cancer Res. 2012; 72(9):2162–71. [PubMed: 22549946]
16. Zhang L, Conejo-Garcia JR, Katsaros D, Gimotty PA, Massobrio M, Regnani G, et al. Intratumoral T Cells, Recurrence, and Survival in Epithelial Ovarian Cancer. New England Journal of Medicine. 2003; 348(3):203–13. [PubMed: 12529460]
17. Quinn BA, Xiao F, Bickel L, Martin L, Hua X, Klein-Szanto A, et al. Development of a syngeneic mouse model of epithelial ovarian cancer. J Ovarian Res. 2010; 3:24. [PubMed: 20958993]
18. Gritsina G, Xiao F, O'Brien SW, Gabbasov R, Maglaty MA, Xu RH, et al. Targeted Blockade of JAK/STAT3 Signaling Inhibits Ovarian Carcinoma Growth. Mol Cancer Ther. 2015; 14(4):1035–47. [PubMed: 25646015]
19. Do TV, Xiao F, Bickel LE, Klein-Szanto AJ, Pathak HB, Hua X, et al. Aurora kinase A mediates epithelial ovarian cancer cell migration and adhesion. Oncogene. 2014; 33(5):539–49. [PubMed: 23334327]
20. Xu S, Yang Yn, Dong L, Qiu W, Yang L, Wang X, et al. Construction and characteristics of an E-cadherin-related three-dimensional suspension growth model of ovarian cancer. Scientific reports. 2014; 4:5646. [PubMed: 25008268]
21. Nikonova AS, Gaponova AV, Kudinov AE, Golemis EA. CAS proteins in health and disease: An update. IUBMB Life. 2014; 66(6):387–95. [PubMed: 24962474]
22. Izumchenko E, Singh MK, Plotnikova OV, Tikhmyanova N, Little JL, Serebriiskii IG, et al. NEDD9 promotes oncogenic signaling in mammary tumor development. Cancer Res. 2009; 69(18):7198–206. [PubMed: 19738060]
23. Singh MK, Izumchenko E, Klein-Szanto AJ, Egleston BL, Wolfson M, Golemis EA. Enhanced genetic instability and dasatinib sensitivity in mammary tumor cells lacking NEDD9. Cancer Res. 2010; 70(21):8907–16. [PubMed: 20940402]
24. Ma Y, Ma L, Guo Q, Zhang S. Expression of bone morphogenetic protein-2 and its receptors in epithelial ovarian cancer and their influence on the prognosis of ovarian cancer patients. J Exp Clin Cancer Res. 2010; 29:85. [PubMed: 20587070]
25. Siu MK, Wong ES, Kong DS, Chan HY, Jiang L, Wong OG, et al. Stem cell transcription factor NANOG controls cell migration and invasion via dysregulation of E-cadherin and FoxJ1 and contributes to adverse clinical outcome in ovarian cancers. Oncogene. 2013; 32(30):3500–9. [PubMed: 22945654]

26. Okada A, Ohta Y, Brody SL, Watanabe H, Krust A, Chambon P, et al. Role of foxj1 and estrogen receptor alpha in ciliated epithelial cell differentiation of the neonatal oviduct. J Mol Endocrinol. 2004; 32(3):615–25. [PubMed: 15171704]
27. Thomas J, Morle L, Soulavie F, Laurencon A, Sagnol S, Durand B. Transcriptional control of genes involved in ciliogenesis: a first step in making cilia. Biol Cell. 2010; 102(9):499–513. [PubMed: 20690903]
28. Bowen NJ, Logani S, Dickerson EB, Kapa LB, Akhtar M, Benigno BB, et al. Emerging roles for PAX8 in ovarian cancer and endosalpingeal development. Gynecol Oncol. 2007; 104(2):331–7. [PubMed: 17064757]
29. Natraj U, Bhatt P, Vanage G, Moodbidri SB. Overexpression of monkey oviductal protein: purification and characterization of recombinant protein and its antibodies. Biol Reprod. 2002; 67(6):1897–906. [PubMed: 12444068]
30. Perets R, Drapkin R. It's Totally Tubular…Riding The New Wave of Ovarian Cancer Research. Cancer Research. 2016; 76(1):10–7. [PubMed: 26669862]
31. Wu R, Zhai Y, Kuick R, Karnezis AN, Garcia P, Naseem A, et al. Impact of oviductal versus ovarian epithelial cell of origin on ovarian endometrioid carcinoma phenotype in the mouse. J Pathol. 2016; 240(3):341–51. [PubMed: 27538791]
32. Ben-Porath I, Thomson MW, Carey VJ, Ge R, Bell GW, Regev A, et al. An embryonic stem cell-like gene expression signature in poorly differentiated aggressive human tumors. Nat Genet. 2008; 40(5):499–507. [PubMed: 18443585]
33. Schwede M, Spentzos D, Bentink S, Hofmann O, Haibe-Kains B, Harrington D, et al. Stem Cell-Like Gene Expression in Ovarian Cancer Predicts Type II Subtype and Prognosis. PLoS One. 2013; 8(3):e57799. [PubMed: 23536770]
34. Kessler M, Hoffmann K, Brinkmann V, Thieck O, Jackisch S, Toelle B, et al. The Notch and Wnt pathways regulate stemness and differentiation in human fallopian tube organoids. Nat Commun. 2015; 6:8989. [PubMed: 26643275]
35. Munoz J, Stange DE, Schepers AG, van de Wetering M, Koo BK, Itzkovitz S, et al. The Lgr5 intestinal stem cell signature: robust expression of proposed quiescent '+4' cell markers. Embo J. 2012; 31(14):3079–91. [PubMed: 22692129]
36. Ice RJ, McLaughlin SL, Livengood RH, Culp MV, Eddy ER, Ivanov AV, et al. NEDD9 depletion destabilizes Aurora A kinase and heightens the efficacy of Aurora A inhibitors: implications for treatment of metastatic solid tumors. Cancer Res. 2013; 73(10):3168–80. [PubMed: 23539442]
37. Ji H, Ramsey MR, Hayes DN, Fan C, McNamara K, Kozlowski P, et al. LKB1 modulates lung cancer differentiation and metastasis. Nature. 2007; 448(7155):807–10. [PubMed: 17676035]
38. Kim M, Gans JD, Nogueira C, Wang A, Paik JH, Feng B, et al. Comparative oncogenomics identifies NEDD9 as a melanoma metastasis gene. Cell. 2006; 125(7):1269–81. [PubMed: 16814714]
39. Natarajan M, Stewart JE, Golemis EA, Pugacheva EN, Alexandropoulos K, Cox BD, et al. HEF1 is a necessary and specific downstream effector of FAK that promotes the migration of glioblastoma cells. Oncogene. 2006; 25(12):1721–32. [PubMed: 16288224]
40. Minn AJ, Gupta GP, Siegel PM, Bos PD, Shu W, Giri DD, et al. Genes that mediate breast cancer metastasis to lung. Nature. 2005; 436(7050):518–24. [PubMed: 16049480]
41. Seo S, Nakamoto T, Takeshita M, Lu J, Sato T, Suzuki T, et al. Crk-associated substrate lymphocyte type regulates myeloid cell motility and suppresses the progression of leukemia induced by p210Bcr/Abl. Cancer science. 2011; 102(12):2109–17. [PubMed: 21848808]
42. Wang Z, Shen M, Lu P, Li X, Zhu S, Yue S. NEDD9 may regulate hepatocellular carcinoma cell metastasis by promoting epithelial-mesenchymal-transition and stemness via repressing Smad7. Oncotarget. 2016; 8(1)
43. Ratushny V, Pathak HB, Beeharry N, Tikhmyanova N, Xiao F, Li T, et al. Dual inhibition of SRC and Aurora kinases induces postmitotic attachment defects and cell death. Oncogene. 2012; 31(10):1217–27. [PubMed: 21785464]
44. Silver DL, Naora H, Liu J, Cheng W, Montell DJ. Activated signal transducer and activator of transcription (STAT) 3: localization in focal adhesions and function in ovarian cancer cell motility. Cancer Res. 2004; 64(10):3550–8. [PubMed: 15150111]

45. Ward KK, Tancioni I, Lawson C, Miller NL, Jean C, Chen XL, et al. Inhibition of focal adhesion kinase (FAK) activity prevents anchorage-independent ovarian carcinoma cell growth and tumor progression. Clinical & experimental metastasis. 2013; 30(5):579–94. [PubMed: 23275034]

46. Wiener JR, Windham TC, Estrella VC, Parikh NU, Thall PF, Deavers MT, et al. Activated Src Protein Tyrosine Kinase Is Overexpressed in Late-Stage Human Ovarian Cancers. Gynecologic Oncology. 2003; 88(1):73–9. [PubMed: 12504632]

47. Sivertsen S, Berner A, Michael CW, Bedrossian C, Davidson B. Cadherin expression in ovarian carcinoma and malignant mesothelioma cell effusions. Acta cytologica. 2006; 50(6):603–7. [PubMed: 17152269]

48. Kulbe H, Chakravarty P, Leinster DA, Charles KA, Kwong J, Thompson RG, et al. A dynamic inflammatory cytokine network in the human ovarian cancer microenvironment. Cancer Res. 2012; 72(1):66–75. [PubMed: 22065722]

49. Zhong J, Baquiran JB, Bonakdar N, Lees J, Ching YW, Pugacheva E, et al. NEDD9 stabilizes focal adhesions, increases binding to the extra-cellular matrix and differentially effects 2D versus 3D cell migration. PLoS One. 2012; 7(4):e35058. [PubMed: 22509381]

50. Fuller E, Howell V. Culture Models to Define Key Mediators of Cancer Matrix Remodeling. Frontiers in Oncology. 2014; 4(57)

51. Buchheit CL, Weigel KJ, Schafer ZT. Cancer cell survival during detachment from the ECM: multiple barriers to tumour progression. Nat Rev Cancer. 2014; 14(9):632–41. [PubMed: 25098270]

52. Little JL, Serzhanova V, Izumchenko E, Egleston BL, Parise E, Klein-Szanto AJ, et al. A requirement for Nedd9 in luminal progenitor cells prior to mammary tumorigenesis in MMTV-HER2/ErbB2 mice. Oncogene. 2014; 33(4):411–20. [PubMed: 23318423]

53. Beck TN, Chikwem AJ, Solanki NR, Golemis EA. Bioinformatic approaches to augment study of epithelial-to-mesenchymal transition in lung cancer. Physiological Genomics. 2014; 46(19):699–724. [PubMed: 25096367]

54. Paik DY, Janzen DM, Schafenacker AM, Velasco VS, Shung MS, Cheng D, et al. Stem-like epithelial cells are concentrated in the distal end of the fallopian tube: a site for injury and serous cancer initiation. Stem cells. 2012; 30(11):2487–97. [PubMed: 22911892]

55. Connolly DC, Hensley HH. Xenograft and transgenic mouse models of epithelial ovarian cancer and non-invasive imaging modalities to monitor ovarian tumor growth in situ: applications in evaluating novel therapeutic agents. Curr Protoc Pharmacol. 2009 Chapter 14:Unit14 2.

56. Liu H, Xiao F, Serebriiskii IG, O'Brien SW, Maglaty MA, Astsaturov I, et al. Network Analysis Identifies an HSP90-Central Hub Susceptible in Ovarian Cancer. Clinical Cancer Research. 2013; Published OnlineFirst July 30, 2013. doi: 10.1158/1078-0432

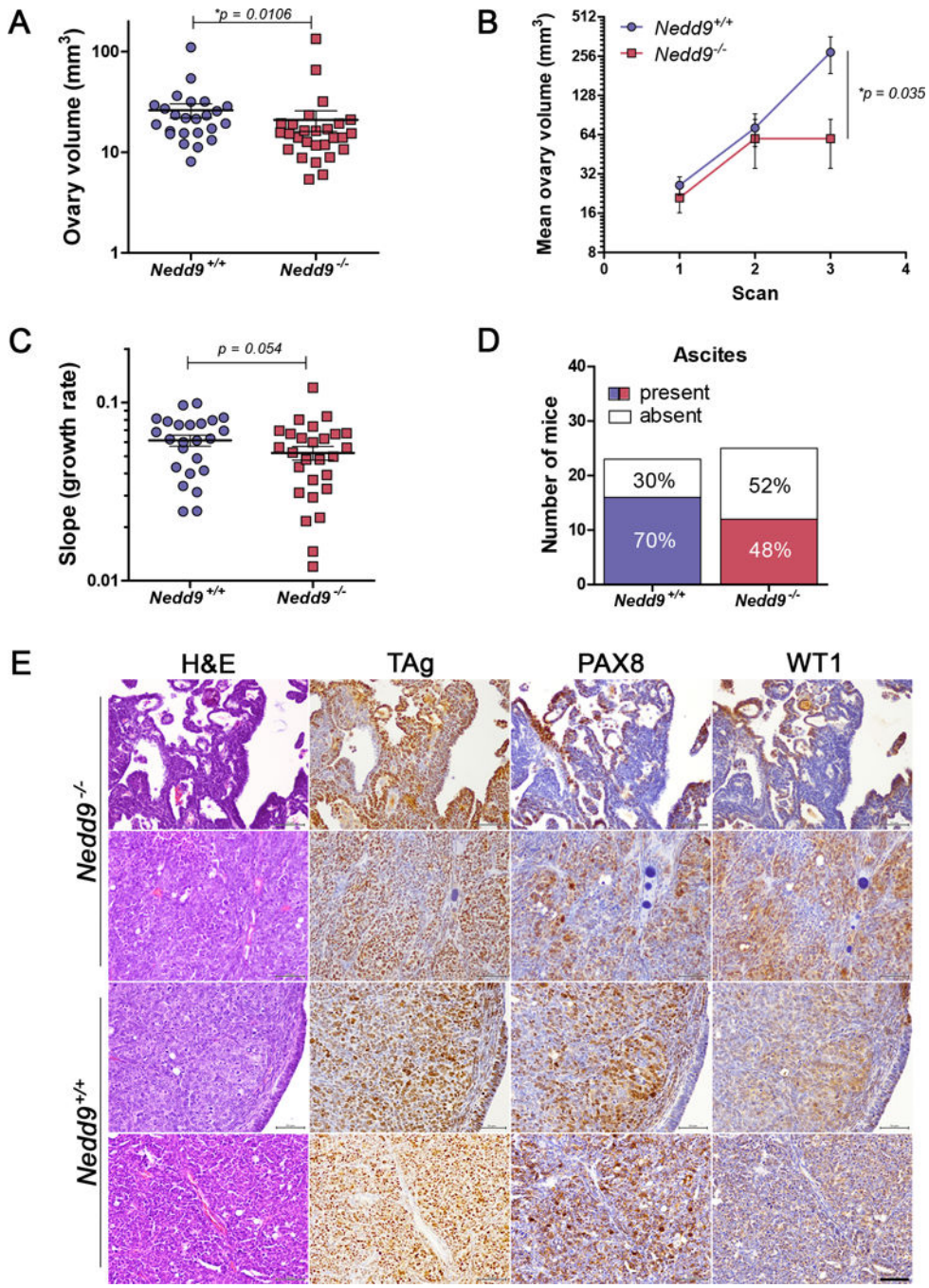

Figure 1. Spontaneous ovarian tumor growth in *MISIIR-TAg;Nedd9*$^{+/+}$ and *MISIIR-TAg;Nedd9*$^{-/-}$ transgenic mice

A) Initial ovarian tumor volume determined in baseline MRI scans of age matched female *MISIIR-TAg;Nedd9*$^{+/+}$ (n=24, average age 80.96 days) and *MISIIR-TAg;Nedd9*$^{-/-}$ (n=27, average age 79.3 days) mice shows mean tumor volume is lower in *MISIIR-TAg;Nedd9*$^{-/-}$ mice. The numbers of randomly selected mice for each genotype were based on the known variability of the spontaneous tumor induction and latency of the *MISIIR-TAg* model. **B)** Tumor volumes calculated from the first three consecutive MRI datasets, when all mice in

both cohorts were alive and of comparable mean age at each scan. By the third scan, *MISIIR-TAg;Nedd9*$^{-/-}$ mice show significantly decreased mean log-transformed tumor volume compared to *MISIIR-TAg;Nedd9*$^{+/+}$ mice at comparable ages (n=24, average age 111.9 days vs. n=27 mice, average age 109.7 days). **C)** Longitudinal MRI datasets from all *MISIIR-TAg;Nedd9*$^{+/+}$ (n=24) and *MISIIR-TAg;Nedd9*$^{-/-}$ (n=27) mice were used to determine the ovarian tumor volume at each scan for all mice on study. The growth rate (log-transformed growth slope) was calculated for each individual mouse and showed a delay in *MISIIR-TAg;Nedd9*$^{-/-}$ mice (mean slope=0.0521) compared to *MISIIR-TAg;Nedd9*$^{+/+}$ controls (mean slope=0.0612). **D)** The number of mice with ascites detected at necropsy was reduced in the *MISIIR-TAg;Nedd9*$^{-/-}$ compared to *MISIIR-TAg;Nedd9*$^{+/+}$ mice. **E)** Ovarian tumors from *MISIIR-TAg;Nedd9*$^{-/-}$ and *MISIIR-TAg;Nedd9*$^{+/+}$ mice collected at study endpoint and paraffin embedded sections were stained with H&E, TAg, PAX8 and WT1. Representative images from tissues isolated from *MISIIR-TAg;Nedd9*$^{-/-}$ mice #129 (163 days) and 195 (204 days) and *MISIIR-TAg;Nedd9*$^{+/+}$ mice #7509 (135 days) and 7431 (181 days) are shown (scale bar=50μm). Ovarian volumes at baseline scans were analyzed by the nonparametric two-tailed Wilcoxon-Mann-Whitney test. Tumor volume data were analyzed using linear mixed-effects models with random intercepts to model longitudinal log-transformed volume data from the first three time points. Individual tumor growth rates throughout the study were analyzed by the two-tailed Wilcoxon signed-rank test. Results are shown as mean ± s.e.m. Investigators were blinded to the genotype of the mice for MRI imaging and analysis of tumor volume.

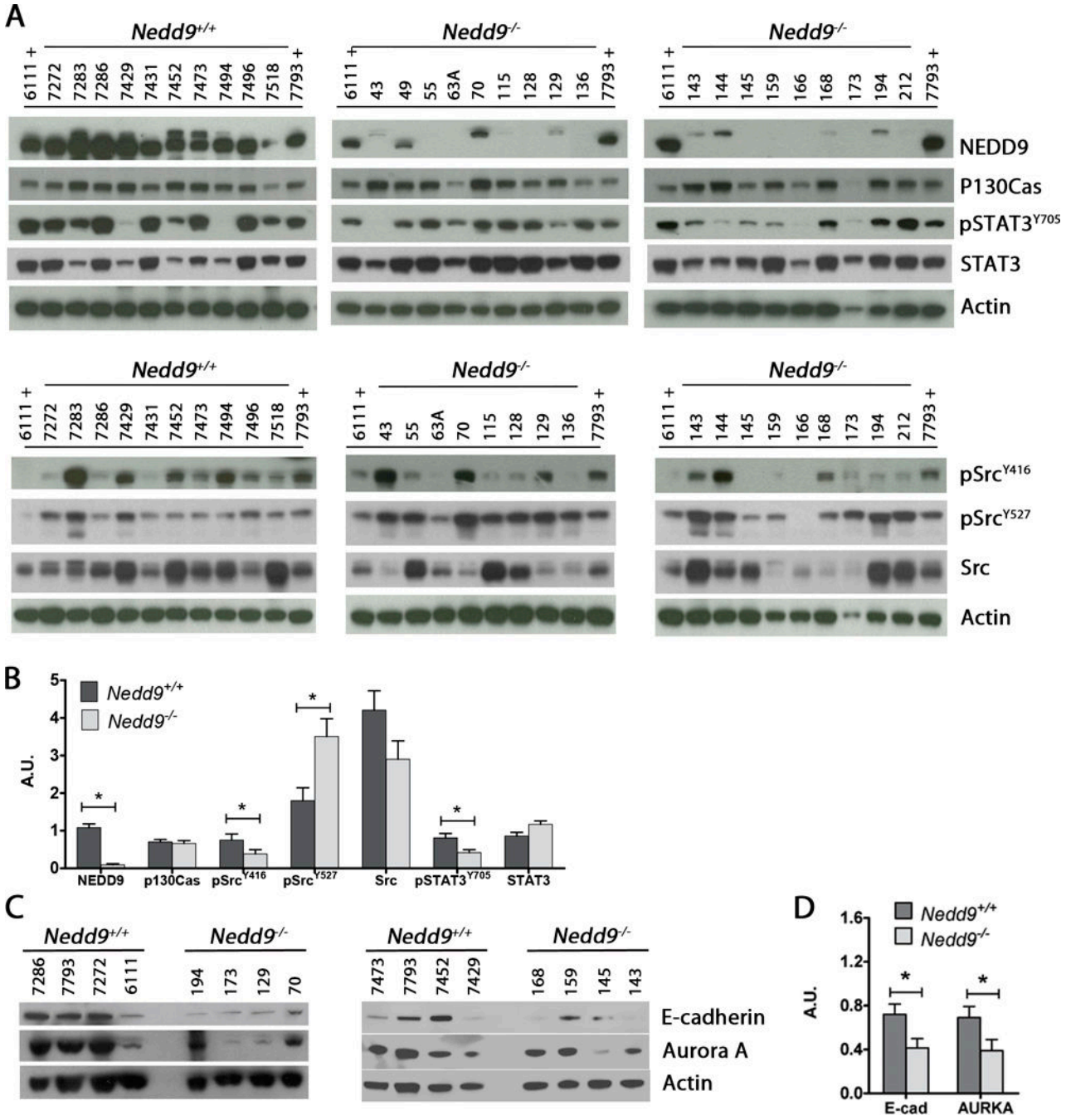

Figure 2. Expression and activation of oncogenic signaling in *Nedd9* wild type and null ovarian tumors

A) Western blot analysis of snap frozen tumor tissue lysates shows the level of expression and/or activation of indicated oncogenic proteins. Samples labeled with '+' are reference specimens loaded on all gels for cross comparison. **B)** Densitometric analysis of the representative immunoblot images to show NEDD9 (upper band on the NEDD9 blot is non-specific), Src, pSRC, STAT3, pSTAT3, E-Cadherin and AURKA levels relative to β-actin. Representative western blots from 3 experiments (arbitrary number of samples). Densitometric analysis was performed using Image J and analyzed by the nonparametric

two-tailed Wilcoxon-Mann-Whitney test. Bars labeled with asterisks are statistically significant ($^{*}P<0.05$) and results are summarized as mean ± s.e.m.

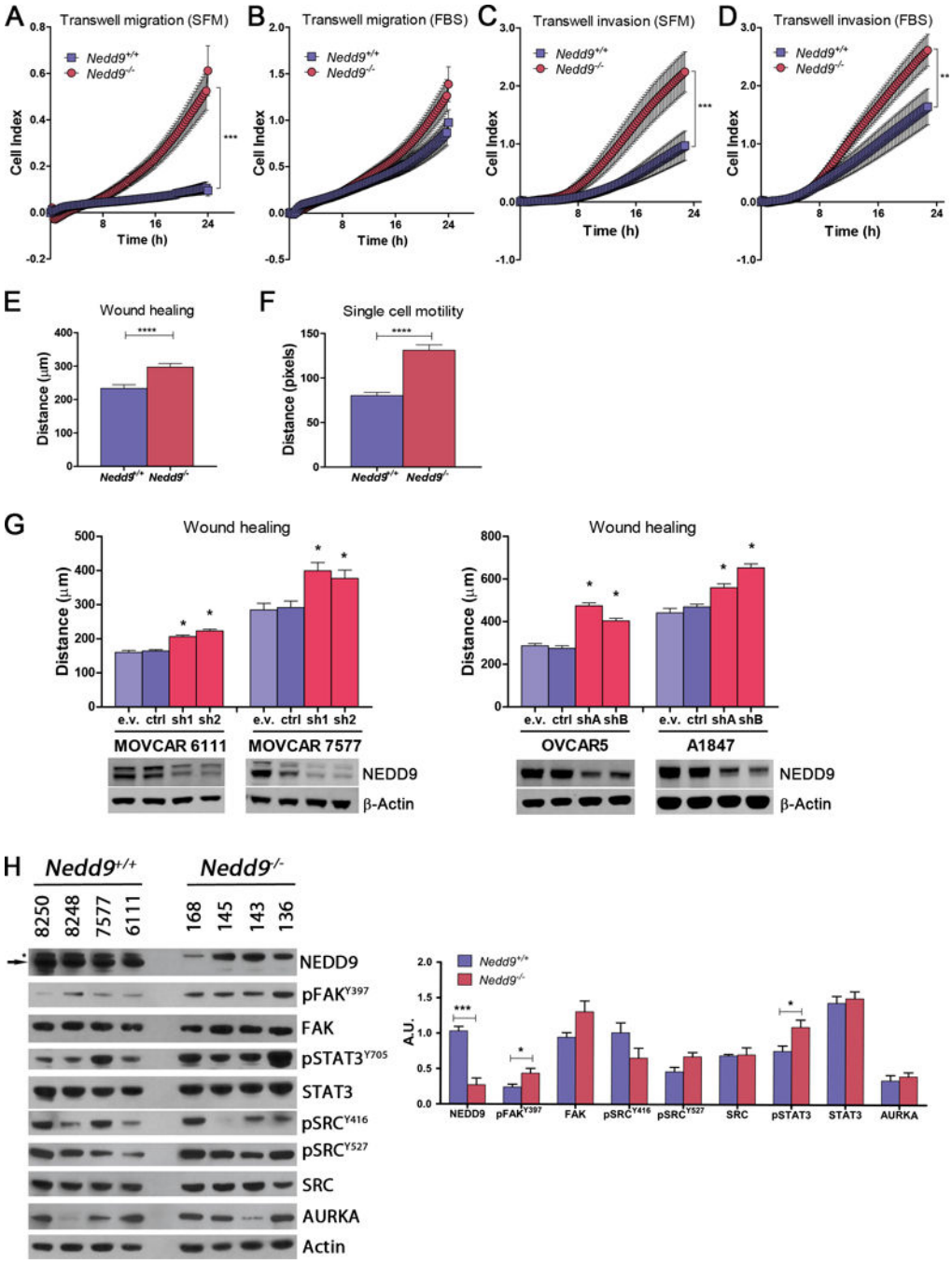

Figure 3. Effects of *Nedd9* loss or depletion on *in vitro* migration and invasion of OC cells

Four independent MOVCAR cell lines established from *Nedd9*$^{+/+}$ (MOVCAR-6111, -7577, -8248 and -8250) and *Nedd9*$^{-/-}$ (MOVCAR-136, -143, -145 and -168) tumor bearing mice were assayed for migration and invasion using transwell migration, transwell invasion, wound healing and single cell motility assays and the mean values are shown for each assay. **A)** Average transwell migration rate was significantly increased in *Nedd9*$^{-/-}$ cell lines in the absence serum (SFM). **B)** No significant differences in transwell migration were detected in the presence of serum. **C-D)** transwell invasion through matrigel was increased in *Nedd9*$^{-/-}$

cell lines in the absence (C) and presence (D) of serum. **E-F)** Wound closure (E) and single cell motility (F) was also significantly increased in *Nedd9*$^{-/-}$ cell lines. **G)** Depletion *NEDD9* in murine (MOVCAR-6111 and -7577) or human (OVCAR-5 and A1847) ovarian carcinoma cell lines by RNA interference (RNAi) with two independent *NEDD9* targeting short hairpin RNAs (shRNA) resulted in more rapid would closure. Depletion of NEDD9 was confirmed by western blotting with anti-NEDD9 antibody and anti-β-Actin antibody as a loading control. All assays were performed in triplicate, analyzed by the nonparametric two-tailed Wilcoxon-Mann-Whitney test and bars labeled with asterisks are statistically significant ($^{*}P<0.05$, $^{***}P<0.001$, $^{****}P<0.0001$, n.s. = not significant). **H)** Expression of a number of proteins interacting with NEDD9 was assessed by Western blot analysis and demonstrated elevation of pFAK^{Y397} and pSTAT3^{Y705} in *Nedd9*$^{-/-}$ MOVCAR cells. The anti-NEDD9 antibody recognizes the 105 kDa NEDD9 protein (indicated by the arrow) as well as a non-specific higher molecular weight band (115-120 kDa) that is indicated by an asterisk. Charts represent mean values ± s.e.m.

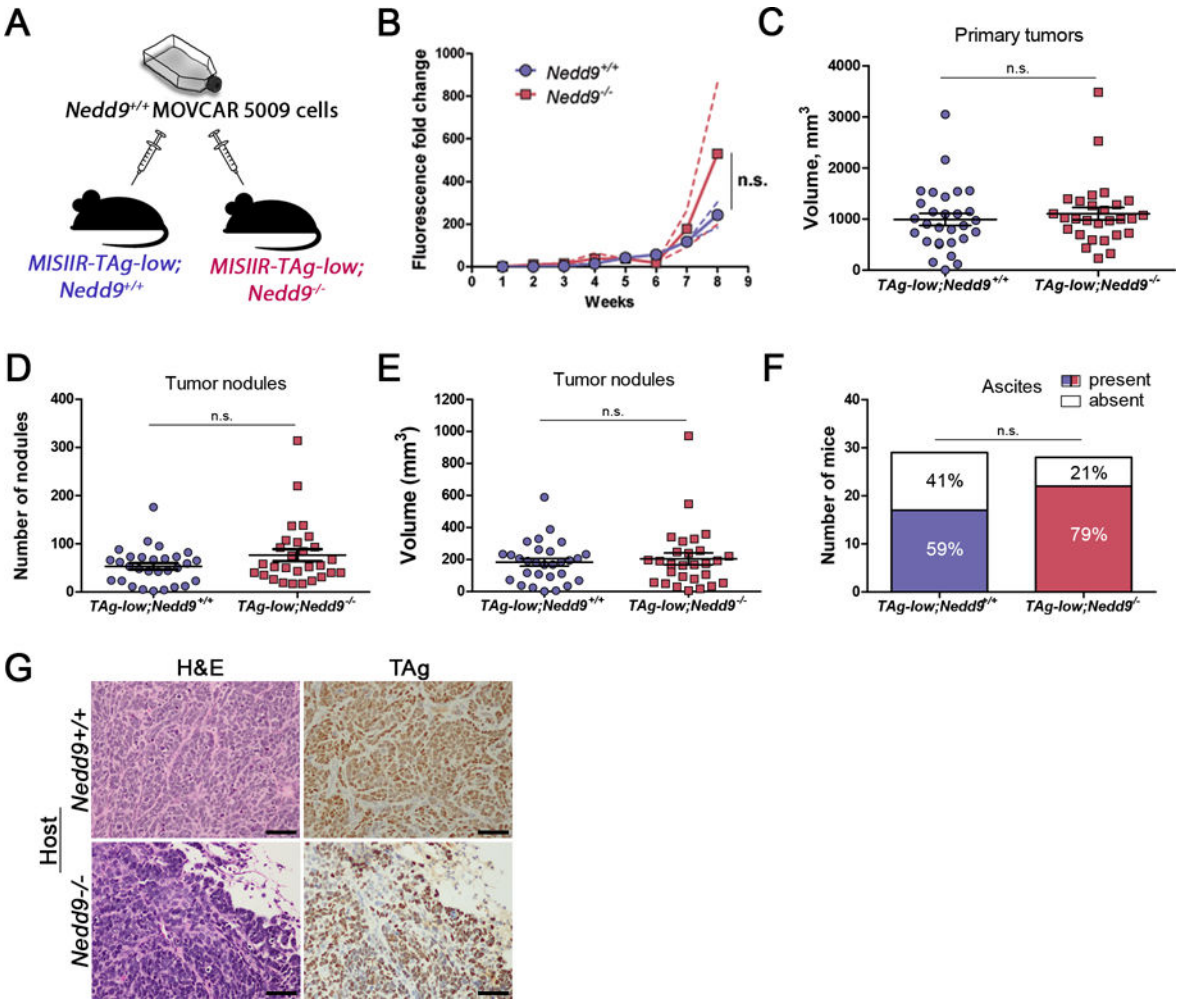

Figure 4. Loss of *Nedd9* in the tumor microenvironment does not impact ovarian tumor growth or dissemination

A) Schematic showing the experimental approach to understand the role of NEDD9 expressed in tumor microenvironment on OC development and progression: *Nedd9*$^{+/+}$ and *Nedd9*$^{-/-}$ *MISIIR-TAg-low* mice were used as hosts for orthotopic (intrabursal) *Nedd9*$^{+/+}$ MOVCAR cell allografts. Investigators were not blinded to the genotype of the allograft host. **B)** Longitudinal bioluminescent imaging (BLI) did not reveal significant effect of *Nedd9*-status on tumor growth rates. **C-F)** Necropsy analysis of tumor allografts grown in *MISIIR-TAg-low;Nedd9*$^{+/+}$ and *MISIIR-TAg-low;Nedd9*$^{-/-}$ hosts showed no significant differences in volume of the primary tumor at the injection site (C) or the number (76.5 ± 12.4 versus 53.3 ± 6.7 tumor nodules) (D) or volume (E) of peritoneal tumor nodules or the incidence (F) of ascites detected. Three independent allograft implantation experiments were performed (n=29 *MISIIR-TAg-low;Nedd9*$^{+/+}$ mice and n=28 *MISIIR-TAg-low;Nedd9*$^{-/-}$ mice in total) and results were analyzed by the nonparametric two-tailed Wilcoxon-Mann-Whitney test for significance. *MISIIR-TAg-low;Nedd9*$^{+/+}$ and *MISIIR-TAg-low;Nedd9*$^{-/-}$ hosts mice were randomly selected for allograft implantation. Charts represent mean values ± s.e.m. G) H&E and TAg stained sections of MOVCAR-5009 allografts grown in *Nedd9*$^{+/+}$ and *Nedd9*$^{-/-}$ *MISIIR-TAg-low* hosts (scale bar=50μm).

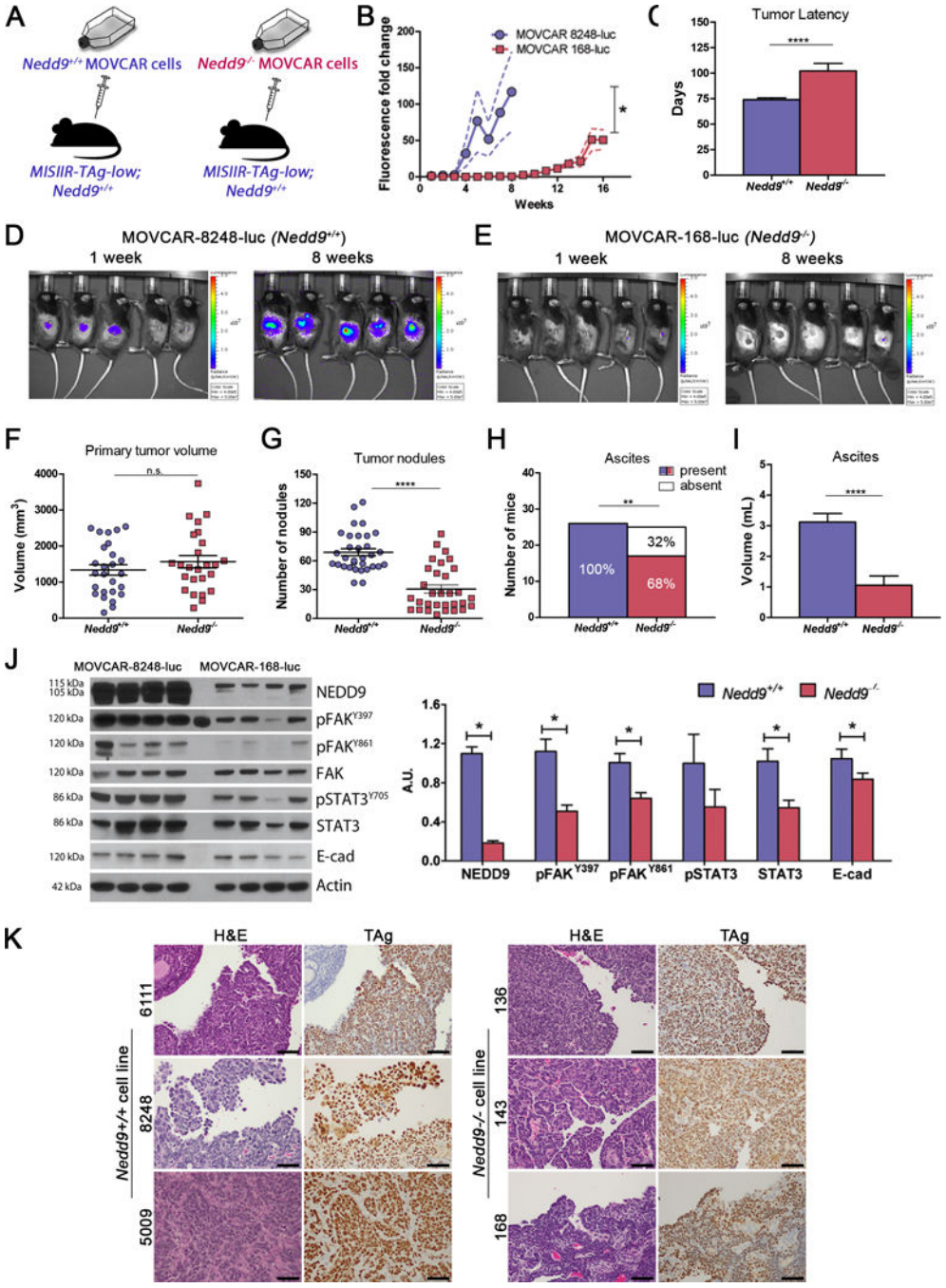

Figure 5. Loss of *Nedd9* in MOVCAR cells impairs OC dissemination

A) Schematic showing the experimental approach to confirm the tumor cell intrinsic role of NEDD9 on OC development and progression: *MISIIR-TAg-low*;*Nedd9*$^{+/+}$ mice selected at random were used as hosts for orthotopic (intrabursal) *Nedd9*$^{+/+}$ (MOVCAR-5009, -6111 and -8248) or *Nedd9*$^{-/-}$ (MOVCAR-136, -143 and -168) cell allografts. Investigators were not blinded to group identity. **B)** Growth of allografts monitored by weekly BLI showing delayed growth in MOVCAR 168-luc (*Nedd9*$^{-/-}$) compared to MOVCAR-8248-luc (*Nedd9*$^{+/+}$) allografts. **C)** Mice were sacrificed when they met humane criteria for euthanasia

and showed significantly increased tumor latency of *Nedd9*$^{-/-}$ allografts compared to *Nedd9*$^{+/+}$ allografts (102.2± 7.4 days versus 74.0 ± 1.8 days for controls, p=0.0004). **D-E)** Representative BLI images showing of MOVCAR-8248 (*Nedd9+/+*) allografts (D) compared to MOVCAR-168 (*Nedd9−/−*) controls (E). **F)** Necropsy analysis of tumor allografts grown in *MISIIR-TAg-low;Nedd9*$^{+/+}$ hosts showed no significant difference in primary tumor at the injection site. **G)** The *Nedd9*$^{-/-}$ allografts exhibited significantly reduced mean number of peritoneal tumor nodules (30.7 ± 4.2 versus 69.0 ± 3.7, p<0.0001), and **H)** the incidence (17/25 [68%] versus 26/26 [100%], p<0.01) and **I)** mean volume (1.06 ml versus 3.12 ml, p<0.0001) of ascites detected. **J)** Immunoblot analysis of tumor lysates confirmed loss of NEDD9 (upper band is non-specific) and decreased activation of oncogenic signaling proteins FAK, STAT3 and E-cadherin in *Nedd9*$^{-/-}$ allografts compared to *Nedd9*$^{+/+}$ controls. The results represent three independent experiments employing three independent *Nedd9*$^{+/+}$ and *Nedd9*$^{-/-}$ MOVCAR cell lines each (n=10 mice/group/experiment). Data were analyzed by the nonparametric two-tailed Wilcoxon-Mann-Whitney test for significance of tumor latency, tumor and ascites volume, and tumor nodules, and the ascites fraction by the Fisher exact 2-sided test ($^{*}P$<0.05, $^{**}P$<0.01, $^{***}P$<0.001, $^{****}P$<0.0001). Representative western blots from MOVCAR-8248 (*Nedd9+/+*) and MOVCAR-168 (*Nedd9−/−*) allograft tumors. Densitometric analysis was performed using Image J and analyzed by the nonparametric two-tailed Wilcoxon-Mann-Whitney test and bars labeled with asterisks are statistically significant ($^{*}P$<0.05). Charts represent mean ± s.e.m. **K)** Representative H&E and TAg stained sections of allograft tumors from *Nedd9*$^{+/+}$ and *Nedd9*$^{-/-}$ MOVCAR cells implanted into *Nedd9*$^{+/+}$ MISIIR-TAg-low mice show similar morphology and TAg staining (scale bar=50μm).

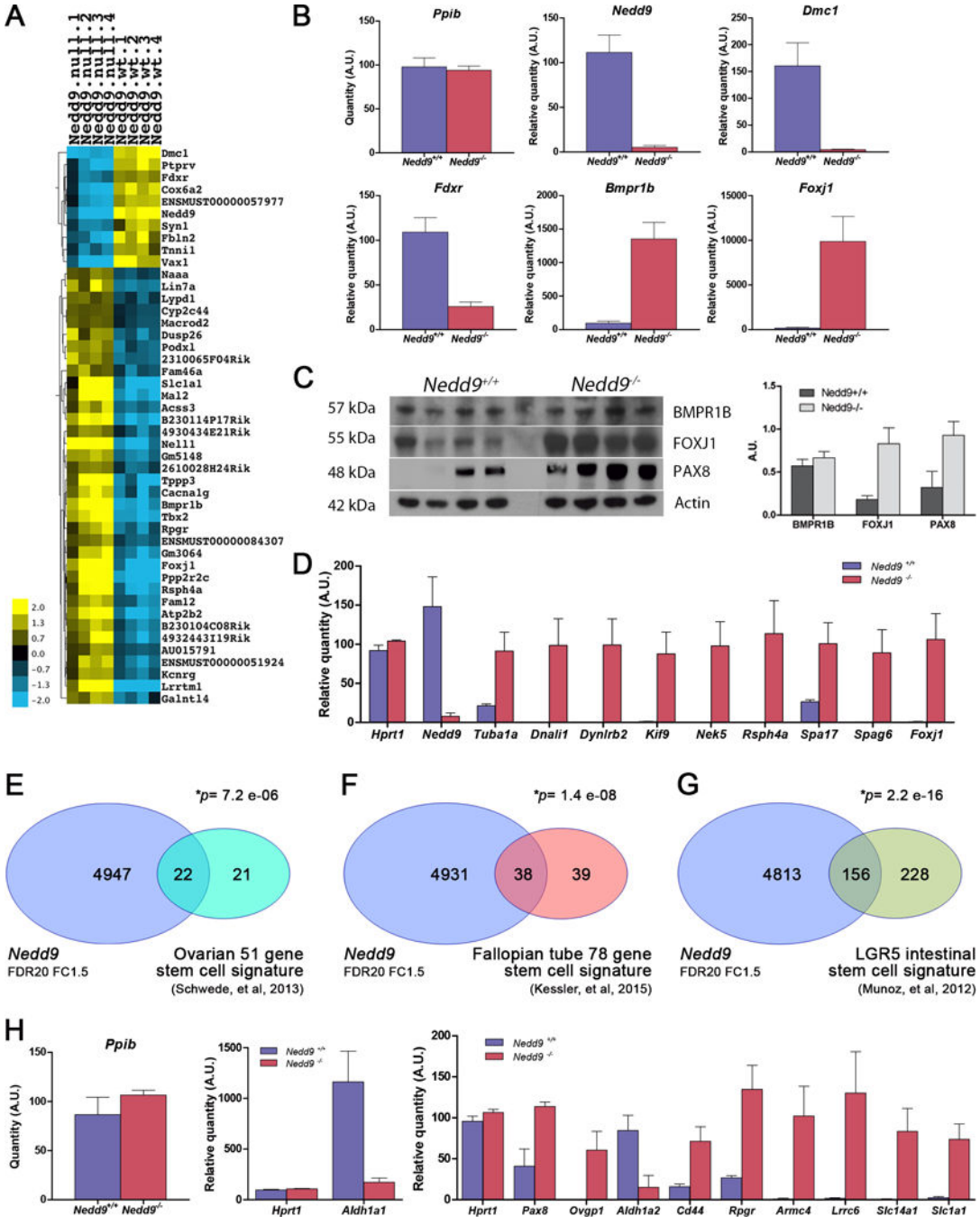

Figure 6. Gene expression differences in *Nedd9*$^{+/+}$ and *Nedd9*$^{-/-}$ tumors

Global gene expression profiles were determined by RNA microarray analysis of *Nedd9*$^{+/+}$ and *Nedd9*$^{-/-}$ tumor specimens, validated by quantitative RT-PCR and compared with publically available data sets. Gene expression data are accessible through Gene Expression Omnibus accession number GSE106911. **A)** Heat map showing 10 downregulated and 36 upregulated RNA probes in tumors isolated from *Nedd9*$^{-/-}$ mice compared to *Nedd9*$^{+/+}$ controls (2-fold change, $p<0.001$ and FDR=5). **B)** Validation of differential gene expression of *Nedd9*, *Dmc1*, *Fdxr*, *Bmpr1b* and *Foxj1* genes in individual tumors by qRT-PCR with

expression of *Ppib* used as a normalizer. **C)** Western blot detection of expression of BMPR1B, FOXJ1 and PAX8 proteins in individual tumors. **D)** Validation of upregulation of FOXJ1 target genes regulating ciliogenesis: *Tuba1a*, *Dnali1*, *Dynlrb2*, *Kif9*, *Nek5*, Rsph4a, Spa17, *Spag6* and *Foxj1* in individual $Nedd9^{-/-}$ tumors by qRT-PCR with expression of *Ppib* and *Hprt1* used as normalizer genes. Overlap of differentially expressed genes in the murine $Nedd9^{+/+}$ and $Nedd9^{-/-}$ gene expression datasets (FDR20, FC1.5) to a 51-gene stem cell-like gene signature in human OC **(E)**, a 78-gene stem cell-associated gene signature in fallopian tube **(F)** and a 384 gene stem cell signature in $LGR5^{+}$ cells in murine intestinal crypt **(G)**. **H)** qRT-PCR validation of individual overlapping genes identified from the above datasets in $Nedd9^{+/+}$ and $Nedd9^{-/-}$ tumors. *Ppib* and *Hprt* were used as normalizer genes for each qRT-PCR experiment. Charts represent mean values ± s.e.m.

Table 1

Average age and tumor volume during early tumor development and at last scan in *Nedd9*$^{+/+}$ and *Nedd9*$^{-/-}$ mice.

	Baseline scan		2nd scan		3rd scan		FINAL Scan	
Genotype	**Mean age (days ± SD)**	**Mean tumor volume (mm^3± SD)**	**Mean age (days ± SD)**	**Mean tumor volume (mm^3± SD)**	**Mean age (days ± SD)**	**Mean tumor volume (mm^3± SD)**	**Mean age (days ± SD)**	**Mean tumor volume (mm^3± SD)**
MISIIR-TAg;Nedd9$^{+/+}$	80.96 ± 17.34	26.16 ± 20.48	96.42 ± 16.71	68.90 ± 101.1	111.9 ± 18.39	274.5 ± 421.0	157.2 ± 23.3	1440.4 ± 617.8
MISIIR-TAg;Nedd9$^{-/-}$	79.30 ± 12.88	21.00 ± 25.34	95.74 ± 16.55	61.34 ± 128.0	109.7 ± 16.59	135.1 ± 283.4	162.2 ± 24.0	1309.9 ± 843.5

Table 2

Summary of endpoint data from longitudinal study of *TgMISIIR-TAg;Nedd9*$^{+/+}$ and *TgMISIIR-TAg;Nedd9*$^{-/-}$ mice.

MISIIR-TAg;Nedd9$^{-/-}$ **mouse ID**	**Age at death (days)**	**Ovary (tumor) volume***	**Ascites**	**Visible spread**	**Microscopic spread**
43	145	756.1	−	+	+
49	153	946.0	−	−	+
55	148	1208.9	−	−	+
63A	182	1581.6	+	+	+
70	192	2284.1	+	+	+
94	130	122.7	−	−	+
115	141	691.4	+	+	+
128	151	35.4	−	+	+
129	163	1843.6	+	+	+
136	138	1255.0	−	+	+
143	188	730.3	−	+	+
144	163	1765.5	+	+	+
145	188	1889.7	+	+	+
146	193	530.5	+	−	+
156	138	1866.8	+	+	+
157	150	181.9	n/a	n/a	n/a
158	200	1748.6	−	−	+
159	158	1289.0	−	+	+
166	138	1680.5	+	+	+
168	150	1912.2	−	+	+
173	118	2563.2	−	−	+
192	183	2717.3	+	−	+
194	191	978.2	+	+	+
195	204	840.5	−	−	+
197	178	25.0	−	−	+
210	156	33.9	n/a	n/a	n/a
212	175	2870.9	+	+	+
***MISIIR-TAg;Nedd9+/+* mouse ID**	**Age at death (days)**	**Ovary (tumor) volume**	**Ascites**	**Visible spread**	**Microscopic spread**

MISIIR-TAg;Nedd9$^{-/-}$ mouse ID	Age at death (days)	Ovary (tumor) volume*	Ascites	Visible spread	Microscopic spread
7272	155	1237.0	no	+	+
7283	175	1615.8	−	−	+
7286	158	642.6	−	−	+
7429	186	947.4	+	+	+
7431	181	1635.0	+	+	+
7452	170	1015.1	−	−	+
7473	159	3125.8	+	+	+
7494	168	783.1	−	+	+
7496	128	33.3	+	+	+
7507	149	1527.9	−	+	+
7509	135	1921.6	−	+	+
7510	128	658.2	+	+	+
7516	209	2267.0	+	+	+
7518	136	1555.9	+	−	+
7523	212	426.4	+	+	+
7524	154	2225.6	n/a	n/a	n/a
7540	146	957.8	−	−	+
7547	157	1973.7	−	+	+
7549	183	1577.9	+	+	+
7555	132	1853.4	−	+	+
7575	137	889.3	−	−	+
7577	207	1356.4	+	−	+
7793	134	1424.4	+	+	+
7859	140	1227.3	−	−	+
7865	149	1725.9	−	−	+
7272	155	1237.0	n/a	n/a	n/a
7283	175	1615.8	+	+	+
7286	158	642.6	−	+	+
7429	186	947.4	−	−	+
7431	181	1635.0	−	−	+

*measurement at last MRI scan

n/a = tissue not available for evaluation